Design of Transduction using NMOS for 3D-Printed NPGF Electrode

A. Arivarasi, Anand Kumar

Abstract— Electrochemical sensors have been tested using voltammetry techniques, which is laboratory based. When the sensor design is of IC packed type with NPGF sensing electrode and to be tested in real time scenario, an effective active transduction is required, showing variation in electric currents from inherent ionic currents. MOSFET based NMOS circuitry serves to transduce the signal having variations for solutions containing various heavy metal ions. NMOS based transduction serves with higher signal to noise ratio, minimal power and compact geometry. Surface resistances for NPGF electrode measures 369 and 560 milliohms. While 18 pico amps are measured for 360 milliohms resistance, 14 pico amps are recorded for 560 milliohms. The variation in electric current values are corresponding to ionic current of inherent NPGF sheet resistances.

.

Keywords— MOSFET, variable resistance, simulation, transduction.

I. Introduction

The term ‘chemical micro sensor’ may be termed as the last phase in a chain of progressive mechanical micro facilities for a complex electromechanical gadget that started as a laboratory scale chemical analytical instrument [1].

This work is carried out in BITS PILANI DUBAI CAMPUS, DUBAI, UAE. There is no funding source involved.

A Arivarasi is with the BITS PILANI DUBAI CAMPUS, Academic city, Dubai. P.O. BOX 345055 Phone +971 04 420 0700 email p20140002@dubai.bits-pilani.ac.in

Anand Kumar is with BITS PILANI DUBAI CAMPUS, Dubai. P.O.BOX 345055 Phone +971 04 420 0700 email akumar@dubai.bits-pilani.ac.in

The analytes are made in contact with the surface of working electrode (modified with self-assembled mono layer). The receptor signal is the ionic chemical current, defined through Randles-Sevcik equation through cyclic voltammetry (through electrochemical methods). Not only on the concentration and diffusion, ionic current is also based on simple redox reactions happening on surface. Electrode surface current is limited by diffusion of ionic species [11].

The physical or chemical changes occurring on the electrode surface is tracked through electronic transduction mechanism. Transduction principles play a vital role for sensor outputs. The types of chemical sensors have traversed from chemresistor to Chemical Field Effect Transistor (CHEMFET), Ion Sensitive Field Effect Transistor (ISFET), Enzyme Field Effect Transistor (ENFET) to Optical Surface Plasmon Resonance (SPR). Sensitivity, Selectivity, robustness, power, size and overhead are the key performance parameters [12].

A chemical sensor consists of a chemical recognition phase coupled with a transduction element. As shown in Figure 1, the receptor part of sensor transforms the chemical energy into the form, a transducer can measure. e.g., Charge. Receptor part might have options that include physical, chemical or biochemical etc., Here the charge due to electron transfers exists as ionic current. The transducer part is a device, which is capable of transforming chemical energy carried by analyte to useful analytical signal [3]. Based on the transducer operation, the chemical sensors are classified as optical, electrochemical, mass sensitive, electrical etc., when the sensing response

is weak; a transducer along with an amplifier is employed to improve the signal strength.

Thin films are of importance in the process of sensing or transduction, where the sensor response increases with decrease in sensing layer thickness. The influence of film thickness was investigated by using such thin films of various thicknesses (80-300 nm) [4]. Micro sensor is the transduction technology where it is based on either micro-fabrication technology or miniaturization technique and takes care of sensitivity, stability and accuracy. Transducers are classified based on the operating principle of receptor mechanism as provided in Figure 2. Each of the methodology is adopted according to the receptor signal property that can be suitably implemented with.

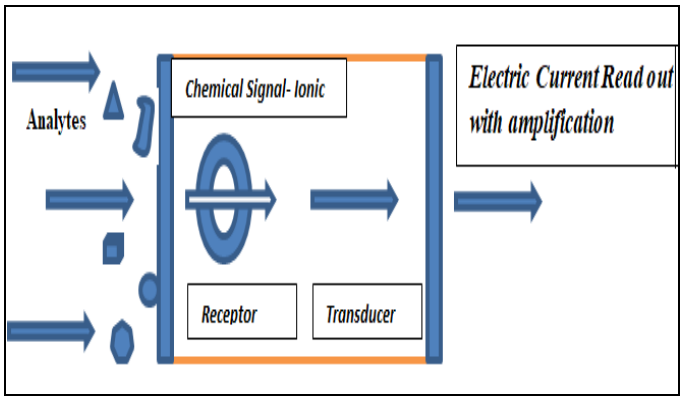

Figure 1: Schematic representation of the function of an electrochemical sensor.

This paper deals with simulation of proposed transduction concept with phenomenon simulation in PSPICE tool. The variable resistance is simulated for its output variant in current, where the Nano Porous Gold Electrode (NPGF) is 3D printed using the simulation analysis Metal Oxide Field Effect Transistor (MOSFET) based transduction process with varying NPGF resistances. MOSFET [21] also amplifies the signal along with effective noise suppression. Analysis of noise in circuit output is also recorded. Hence an active transduction is recommended for heavy metal sensing electrode. The NPGF electrode is 3D printed using modified FDM methodology. Immersion process of electroless plating is automated into a 3D printing process. For the sensor applications, high surface area to volume is key requirement, which can also be utilized for stress changes, resistivity changes, transport of ions. The self assembly of monolayers on top of an electrode can enhance the response or make the detection more selective towards a particular detecting mechanism.

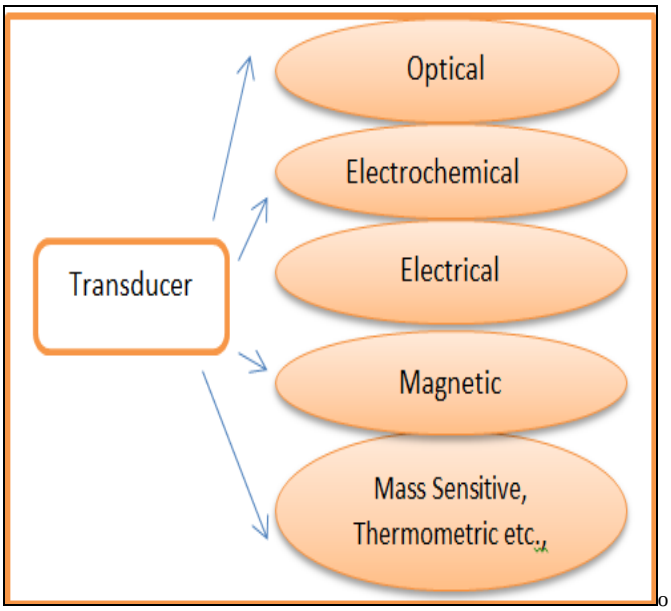

Figure 2. Classification of chemical sensors according to operating principle of receptor / transducer mechanism. Classification of chemical sensors according to operating principle of receptor / transducer mechanism

Signal from a transducer is typically electronic in nature, whether it is current or voltage or impedance/conductance. The change caused by analyte composition change causes the signal variations. Charge transfer variations also can cause final variations w.r.to ions tested. The surface and ionic interference causes a change in charge potentials on surface. Surface should be receptive to such specific interactions, which determines sensor selectivity or quality. Chemical sensors normally involve physical transducer and a chemically sensitive layer or recognition layer. The thermal, optical or electrical signal acts according to the change in chemical property or signal from the recognition surface. Among the two types amperometric and potentiometric types, amperometric is current signal and potentiometric

produces voltage signal. Amperometric senor produces current signal, which is proportional to the concentration of analyte by faraday's law and the law of mass transport. It possess a linear response with analyte concentration. Broad range of geometries exists for a wider analyte detection using amperometric type. It has small size, low power , high sensitivity, lower price ranges, portable. Ion selective electrodes belong to potentiometric chemical sensor group.

I. RESPONSE DEPENDENCIES

A. Response Dependencies on thickness

The microstructure sensor element has to be well defined with respect to grain size, thickness, pore size and temperature [4]. Sensitivity is related to film thickness.

Sensitivity of the sensor decreases with increasing overlay thickness, where degree of interaction between analyte and sensor ultimately determines the sensitivity and selectivity of the sensor system. Hence, diffusion rate depends on film thickness [5][6]. Variability in conductivity is reported [13] due to the fabrication method and film thickness [18][19].

$$I = Nfad^{1/2}C / \delta \qquad - (1)$$

Equation (1) relates thickness and sensitivity, where N= number of electrons, A=electrode area (cm^2), C=Concentration (in mol cm^{-3}), δ = constant related to diffusion layer thickness. The current reaches steady state after a certain time.

B. Response Dependence on temperature

Temperature plays a major role in response for an electrochemical based sensor or a micro sensor. Wheatstone bridge readout interface for ISFETs were introduced to improve noise performance and temperature compensation. To activate reactions, temperature has to be maintained or increased accordingly in experiments. The temperature is tuned for better sensitivities. Usually for electronic readouts, temperature monitoring and control circuit is employed. Temperature in which MOSFET is operated affects the catalytic properties of a sensor. Experiments have been conducted for MOSFETS working in different temperatures, which are applied in sensors [7]. Temperature control streamlines the limit of detection of electro-chemical sensors.

C. Response Dependence on porosity

Presence of pores enhances the transducing activity on sensor surface. In sensing and signal transduction, apart from external stimuli such as pH, redox potential, temperature, ionic concentration - pore size is an inherent surface feature enhancing transducing feature. Typically presence of nanopores on surface increases the surface to volume ratio of surface substantially. The increase in sensing surface provides better response for specific / selective stimuli. Difference in sensitivities for ordinary metal electrodes and porous surface electrodes are a proven phenomenon.

D. Charge – Transfer Absorption

For a complex to exhibit charge-transfer behavior, one of its components must have electron donating properties and another component must be able to accept electrons. Usually molar absorvities from charge transfer absorption mechanism are greater in the range of 10 Lmol-1 /cm [3].

III. OPERATION

Signal transduction and amplification for the selective and amplified chemical / biological responses involve transport of ions. The process of transduction and amplification is provided in the form of subsequent electronic procedures. Figure 3

explains the logical flow transduction circuit for the electrode is provided in Fig 4. Apart from the three Electrochemical based measurement processes (Potentiometry/Voltammetry or amperometry / Conductometry) which are useful as transduction phenomena, active MOSFET configuration can be used for transduction. An active readout is preferred rather than a wheat stone bridge due to its better signal-to-noise ratio and power consumption. The drawback of active readout is that, the output signal is very small and requires amplification. A common gate MOSFET configuration can be used to address the requirement, as it can serve both as amplifier and read out sensor for detecting the change in resistance (Fig 4). By modulating the gate source voltage, the change in micro-electrode resistance is detected and amplified. In this process, an increase in the resistance would lower the drain current consequently increasing the drain source voltage. A degenerated NMOS (N-type Metal Oxide Semiconductor) transistor will help create a feedback and hence to reduce noise generated out of amplification.

A. Characteristics of resistive sensor with MOSFET

1. Resistive sensors measure the resistance change due to chemical reactions. It is classified under conductometric sensors.
2. Controlling arrays of electrochemical sensors (for detecting many ions)
3. The response commonly reported through electrochemical sensors is the normalized change in surface resistance or change in conductivity measured through four point probe. The result is proportional to the analyte concentration.
4. Using MOSFET, a novel CMOS compatible sensor array based on a combined resitive / chemFET sensor could be fabricated. An array of many sensors is suitable for integrated drive, gain and baseline removal for a micro meter CMOS process.

The sensing materials can be a working electrode, conventionally used in electrochemical processes. The resistance change is proportionally varied to electric current, amplified which is actively read-out.

Figure 3 describes the transducing procedure. The varying resistance from NPGF surface is read out using positioned leads. For experimental reasons, it is read out using four point probe instrumentation. The read out resistances are fed to transducer, where the ionic current is converted to electric current. Many kinds of such transducers and circuitry exists, within which MOSFET based circuits provide higher output efficiency. The amplification provided is of higher efficiency. Signal to noise ratio is higher. The converted electrical signal is fed to display device connected to the circuitry. In case of packaged concept, the output leads are connected to display portals. The display conveys the amount of ions present based on detected electric current. The variation in current peaks for a particular concentration of water is baselined. The required allowed levels of particular ions of interest is cross verified or checked and tolerated levels are displayed. If the current peaks repeats for many such occurences, the repetition counts for too many ions presence. The sequence of detection depends on electrode. Selectivity is determined by SAM layer, whereas if the detected signal repeats itself more than once, number of occurences is counted one after other. It is again automated. For example, if lead is detected, the current peak intimates the presence. On the other hand, if copper is detected, the magnitude of current peak is different. The amplified signal is displayed along with encoded text. ppm level of concentration is tested, where in the current level detected can be of nano or pico amps. The signal is amplified for human visualization and interference. The data is encoded such that the transduced signal is human interferrable. Hence the array of MOSFET

transducers are concatenated to form such amplificiation arrays based on individual detections.

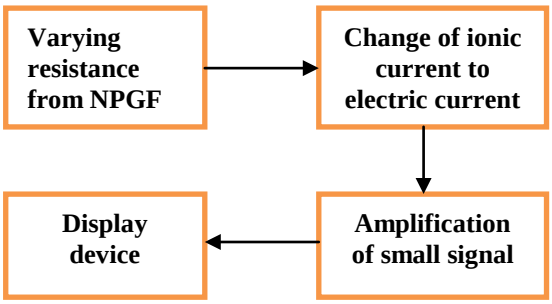

Figure 3 : Block diagram

Nanoporous Gold Film (NPGF) electrode is highly coveted for development of electrodes due to its high electrical conductivity; specific surface to volume ratio; ease of Self Assembled Monolayer (SAM) modification and higher ionic sensitivity. It is used as working electrode for sensing and MEMS applications which also possess mechanical robustness along with surface roughness having porous structure. It is strongly size dependent due to the surface charge driven actuation mechanism [20].

There are multiple steps to fabricate NPGF gold films chemically. NPGF electrodes possess ultrahigh surface area and enhanced electrochemical activity. Excellent selectivity is proved for various heavy metal ion detection. Conventionally it was fabricated by applying multi cyclic potential scans on a polished gold electrode in an electrolyte composed of of $Zncl_2$ and benzyl alcohol. Using the cathodic potential scan, Zn was electrodeposited on the gold electrode surface. Then Au/zn alloy was then formed on the surface under a higher temperature. Nanostructured gold film was produced. NPGF film can also be produced chemically by ebeam evaporation method of producing metal layers. On the other hand, NPGF can also be made by electroless immersion techniques, which can be automated using current printing methodologies.

The change in surface resistance before and after ionic interactions at room temperature is studied. The change in resistance, conductivity varies for different ions of interest. The film consists of highly porous structures with a wide range of internal feature sizes from few to tens of nanometers [8].

Low temperature dealloying method was used to produce nano porous gold. NPGF was synthesized employing a template free and cost effective electroless plating method. The film is transformed into working electrode for electrochemical testing.

The relationship between electrode area, charge resistance and current peak in cyclic voltammetry were analyzed in literature. The number of electrons involved in the redox process of electroactive probe, area of the electrode surface available for the redox process, bulk concentration, diffusion coefficient, processing temperature determines the fabrication operation conditions of gold electrode.

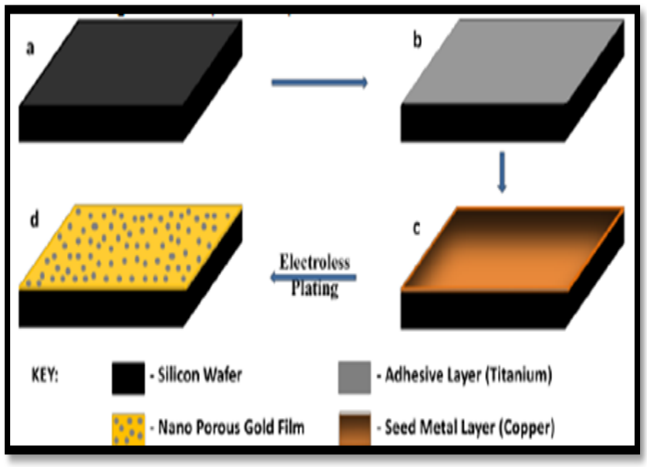

Figure 4: Schematic for NPGF Fabrication through electroless plating [9].

Figure 4 demonstrates the process steps involved in NPGF electroless plating fabrication. 10 nm of thin titanium epoxy layer is designed to use between copper and top layer. Copper is ebeam deposited/electroless deposited, on which the PGC solution is deposited through immersion process [9]. Figure 5 shows the SEM images of both ebeam deposited and electroless plated gold, where the roughness is higher for later. This ensures high

surface area of NPGF, high surface energy and electrochemical sensing activity.

Optical, electrical, surface area are of key considerations to use NPGF. Porous gold films are ideal electrodes for chemical and biological sensor developments. Chemical stability and ease of modification are the key advantages.

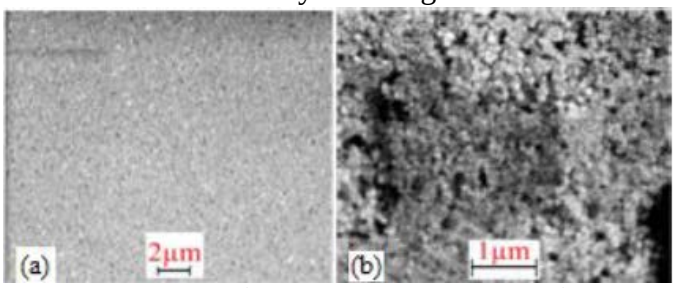

Figure 5: SEM Images of (a) E-beam deposited Au thin film and (b) Electroless plated Au Courtesy: [9]

B. Reference circular shape electrode simulated structure in COMSOL

For the transduction circuit to be connected to the sensing surface, sensor design for testing heavy metal ions is provided. It can be either used as an electrochemical based sensor or as a micro sensor having working electrode packaged with transducing circuit elements.

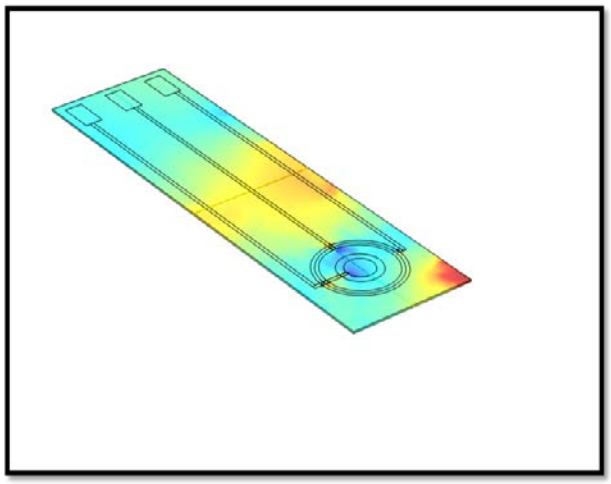

Figure 6: COMSOL Simulation of circular shaped NPGF, designed as in electrochemical sensing set up [22]

The circular shape NPGF is designed and simulated in COMSOL software (Figure 6 and 7), where there are three connections for working, reference and counter electrodes to be used as an electrochemical sensor. Working electrode could be based on NPGF based 3D printed electrode or bismuth nanoparticle coating on carbon.

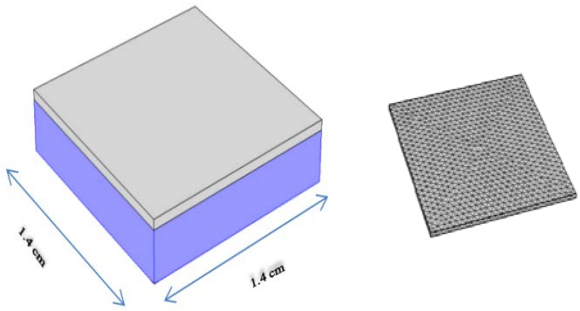

Figure 7: Square shaped NPGF electrode structure designed in COMSOL. Substrate of Si (1.4x1.4cm) is used. Copper surface is shown above. The meshed structure of surface is displayed in (b).

Instead of the circular working electrode, square shaped geometry can be used. Various sensor designs are possible through efficient design methods, depending on packaging area. 3D printing helps in realizing the geometry innovations to reality, where functionalized surface are created by multi material print mechanisms. The geometry, particularly the micro / nano layer resolution are considered for precise printing process. Layering has to be supported for such kinds of printing. Chemical handling is made compatible with modified nozzle mechanism. Individual material supply is carefully handled.

IV. SCHEMATIC OF CMOS COMPATIBLE ACTIVE READOUT

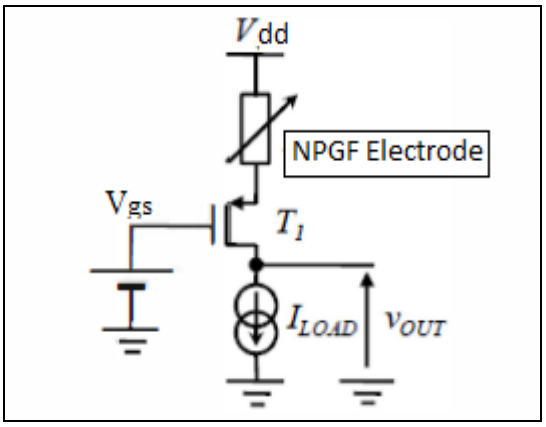

Figure 8: Schematic representation of varying NPGF for transduction through MOSFET

Wheatstone bridge is normally used for readouts, which uses three constant resistances with one variable resistance. The change in resistance is caused due to the sensing elements inducing a voltage change across the bridge, which is then fed to the display system or another unit. Comparing signal to ratio of wheatstone bridge (passive device) and an active readout containing MOSFET, the performances are better for active configuration. Power consumed is much lesser for active device. The drawback of active configuration is that, the output voltage signal is very small and to further utilize the same, there is a need for amplification. Amplification process not only amplifies signal, but also the noise. Hence power consumption gets increased overall. A common gate Metal Oxide Semiconductor (MOS) can be used to address the above issue. It can serve both as as an amplifer and readout sensor. A readout sensor can detect change in resistance of the NPGF electrode due to abdsorption of heavy metal ion like copper. The I_d current is measured [10], where

$$I_{DS} = (W/L)\, C\mu\, [(V_{gs}-V_t - (m/2)V_{ds})]\, V_{ds} \qquad - (2)$$

Where W=Channel width, L=Channel length, C=capacitance, μ=electron surface mobility, V_{gs} = gate source voltage, V_t = threshold voltage, m = constant, V_{ds} = drain source voltage, I_{ds} = drain source current.

The increase or decrease in resistance of electrode (eg. NPGF) due to absorption of heavy metal ions would be amplified by modulating the gate source voltage. Thereby, an increase in resistance would consequently decrease the drain current. Again this will be compensated by drain voltage source increase. NMOS type of MOSFET is used for simulation through PSPICE, so that the noise generated by transistor amplification is reduced. It would normally create a feedback system using degenerative system. The circuit would be encapsulated in a water proof package where only working electrode surface is exposed. Hence the life time will be more with optimized power consumption.

A. Circuit diagram:

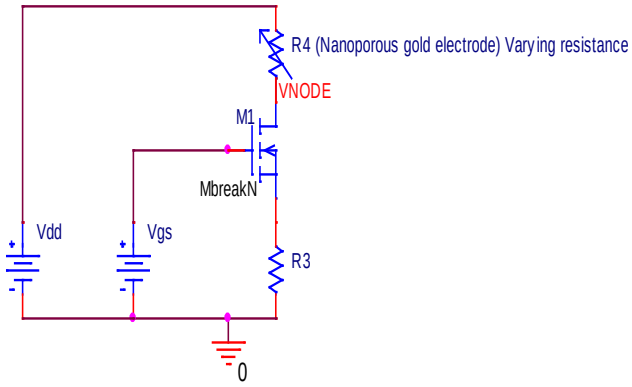

Figure 9: Active read out circuit diagram

In the circuit diagram provided in Figure 8 and 9, MOSFET of type MbreakN transistor is used where Vdd, the drain voltage and Vgs the gate source voltage is provided for drain and gate terminals. Proper grounds are ensured. Here for simulation, NPGF electrodes' experimental measured values are used for resistance values. Varying NPGF resistance from the electrode is connected in drain node. MOSFETs of length 1 μm and width 5 μm are used for simulation in Orcad-Capture Lite. V3 is used for V_{gs} and V2 is for V_{dd} during simulation.

Case 1 –

When V_{gs} = 5 V; R3 = 200 ohms; R1 = 1 kilo ohm

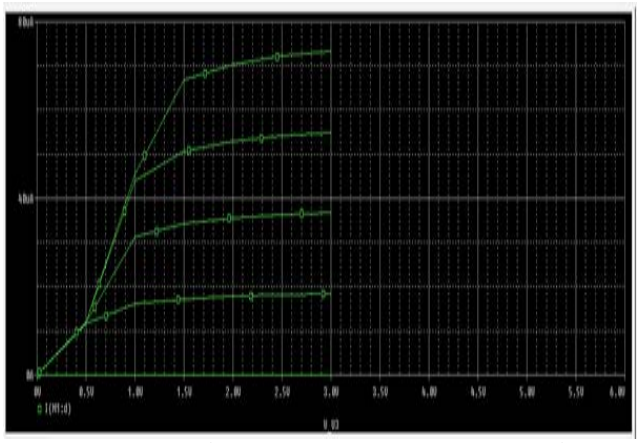

Figure 10: Response of simulated circuit Orcad-capture lite of PSPICE for Vgs Vs Id

Figure 10 demonstrates normal MOSFET operation, when V_{gs} = 5 V for R3 as 200 ohms, with R1 as 1 kilo ohm. For 3D printed NPGF electrode, the variation in resistances are recorded before and after PGC are 560 milliohms and 369 milliohms respectively. The resistance data is used in Pspice simulation to simulate change in output current. DC sweep (primary linear sweep) is performed.

Case 2 : Threshold voltage change (on surface resistance change)

Threshold voltage change is the minimum gate to source voltage difference, which is needed to create conductive path between drain and source. The factors which determine variations during fabrication of device include,

a. Varying doping concentration on substrate
b. Source to body voltage variation
c. Thickness of gate oxide layer

It can be decreased as well vice versa. The plot of V_{gs} Vs I_d is recorded with resistance value as 369 milliohms. The graph is captured for voltage versus current related plot. There is an alteration in threshold voltage drastically (Figure 11). Threshold is varied from *0.5 to 1.2V*. The I_D has changed from 4 micro amps from 4.75 micro amps. Even small changes in threshold voltage are electronically amplified to increase sensitivity. MOSFET design parameters are taken into consideration. NMOS and PMOS processes are designed to have nominal threshold voltages of 0.5 and -0.5 V based on channel implant conditions. Drain and gate bias depends on the threshold voltages. The gate threshold voltage increases approximately linearly with drain voltage, but it may saturate at higher $V_{ds.}$ Drain threshold voltage increases linearly with gate voltage and saturates at a particular $V_{gs.}$ The interdependence of gate and drain control of energy in tunneling area have an important implication in digital arena.

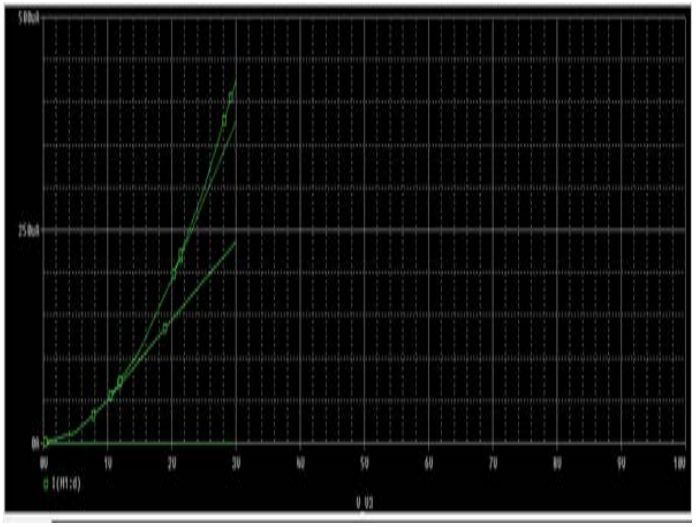

Figure 11: Plot of Vgs Vs Id for R4 as 369 milliohms

Case 3 – Changing the sweep resistance using simulation

When R4 = 1K, R3 =200 ohms, and changing resistance 0 to 1k, the following values are obtained. The value of transistor power is 13.73 mW and at variable resistor lesser dissipation of 47.47 nW is simulated for bias voltages and currents. The biasing current is 3.141 milli amps, even when R4 value is 369 milliohms. 369 and 560 milliohms are the sheet resistances measured through four point probe during experimentation. The same data is used for simuation inorder to track the variation in minor resistances. The ionic current in surface is transformed to electric current/voltage at the output of MOSFET operation. The change in I_d current is tracked, as the drain current plays a main role in load current. If further amplification is

required, amplifiers are added according to the level s of requirement. MOSFET with resistive drain can act as voltage and current amplifier.

Case 3a: For R4 as 560 milliohms

The resistance is set as variable parameter in PSPICE simulation. As sweep resistance (RVAL) changes from 0 to 1K for 560 milliohms surface resistance, the current appropriately changes (decreases) from *3.142 nA towards 3.124 nA (0.018 nA decrease*).

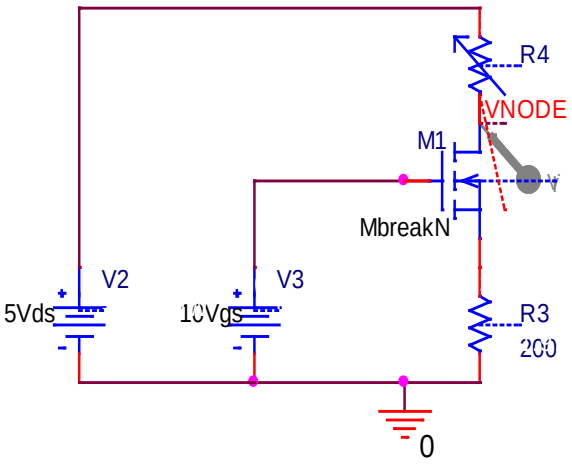

Figure 12a: When changing R4 to 369 milliohms

Again in milliohms range variations, the current remains in 3.142 nano amps (Figure 12 a/b).

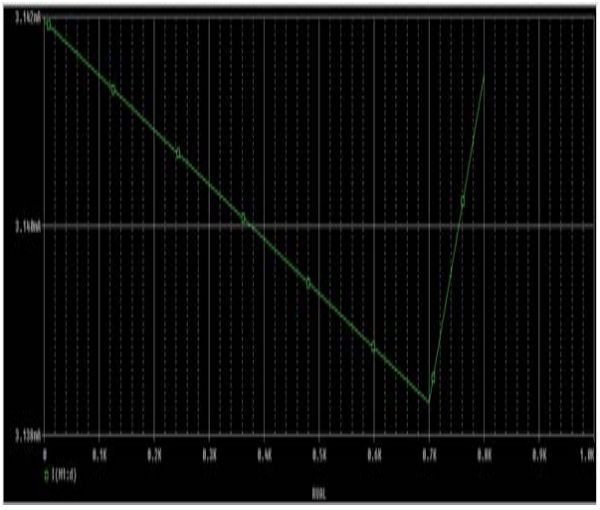

Figure 12b : 560 milliohms current changes in Pspice

Case 3 b: When changing R4 to 369 milliohms

For sweep resistance value changing from 0 to 1k range for 369 milliohms surface resistance, the current decreases as in case 3a. It decreases from *3.142 nA to 3.128 nano amps*. For milli amps change variations in RVAL, 430 µA is measured (Figure 13a/b).

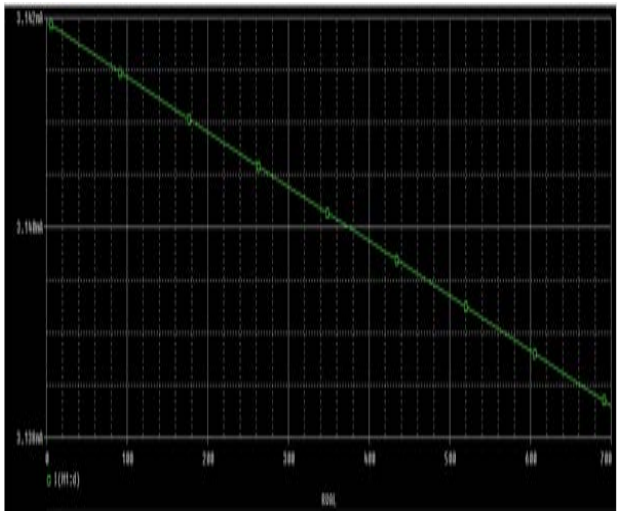

Figure 13a

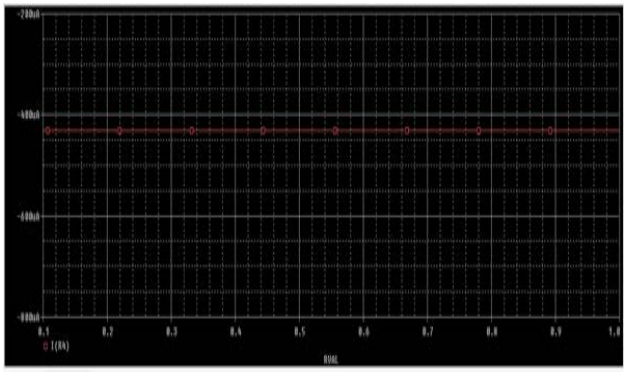

Figure 13b

B. Power Dissipation

The total power dissipation for the circuit is calculated to be 1.57e-02 Watts, which is comparably lesser. Pspice report is provided in Table 1.

Table 1 – Pspice report and net power dissipation at room temperature

Pspice Report

```
                    MOSFET MODEL PARAMETERS
**************************************************

MbreakN
```

```
NMOS
LEVEL    1
L  100.000000E-06
W  100.000000E-06
VTO    0
KP   20.000000E-06
GAMMA    0
PHI     .6
LAMBDA    0
IS   10.000000E-15
JS    0
PB     .8
PBSW     .8
XJ    0
UCRIT   10.000000E+03
DIOMOD    1


SMALL  SIGNAL  BIAS  SOLUTION           TEMPERATURE  =
27.000 DEG C

*****************************************************

NODE   VOLTAGE     NODE   VOLTAGE     NODE   VOLTAGE
NODE   VOLTAGE


(VNODE)    5.0000  (N02592)    5.0000 (N02652)
10.0000 (N026380)     .6283

    VOLTAGE SOURCE CURRENTS
    NAME         CURRENT

    V_V2        -3.141E-03
    V_V3         0.000E+00

    TOTAL POWER DISSIPATION   1.57E-02  WATTS

*****************************************************
```

The power in R4 Resistor changes w.r.to resistor changes as in Figure 14.

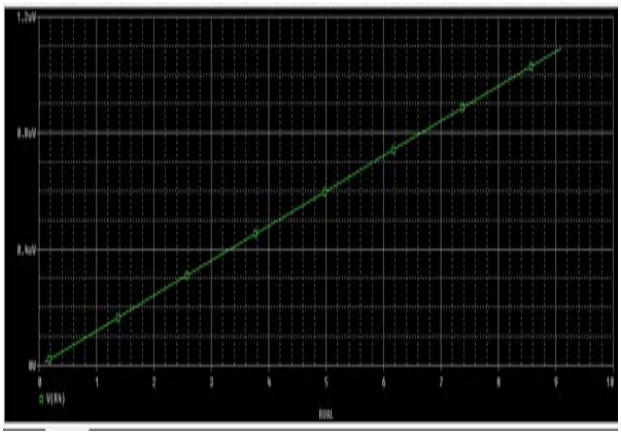

Figure 14 – Changes in power with varying resistance values

The sensitivity (circuit elements) figures are provided in Table 2.

Table 2 - DC SENSITIVITIES OF OUTPUT V(VNODE)

ELEMENT NAME	ELEMENT VALUE (VOLTS/UNIT)	ELEMENT SENSITIVITY (VOLTS/PERCENT)	NORMALIZED SENSITIVITY
R_R3	2.000E+02	2.452E-08	4.904E-08
R_R4	9.890E-03	3.141E-03	3.107E-07
V_V2	5.000E+00	1.000E+00	5.000E-02
V_V3	1.000E+01	-3.641E-06	-3.641E-07

Process analysis specifications are provided underneath.

Simulation Run: 0 (Nominal Run)

Param : V2.DC (V_V2.DC) = 10Vdc

Param : R3.VALUE (R_R3.Value) = 1k

Param:R4.Value (R_R4.Value) = 560 milliohms
Param : V1.DC (V_V1.DC) = 7V
Specs:Max(I(M1:d)) = 431.46184192755248u

Simulation Run: 1

Param : V2.DC (V_V2.DC) = 10.40000000000000

Param : R3.VALUE (R_R3.Value) = 1k

Param : R4.Value (R_R4.Value) = 560 milliohms

Param : V1.DC (V_V1.DC) = 7V

Specs : Max(I(M1:d)) = 431.46184228110337u

Simulation Run: 2

Param : V2.DC (V_V2.DC) = 10Vdc

Param : R3.VALUE (R_R3.Value) = 1.00160000000000k

Param : R4.Value (R_R4.Value) = 560 milliohms

Param : V1.DC (V_V1.DC) = 7V

Specs : Max(I(M1:d)) = 431.38171562586268u

Simulation Run: 3

Param : V2.DC (V_V2.DC) = 10Vdc

Param : R3.VALUE (R_R3.Value) = 1k

Param : R4.Value (R_R4.Value) = 400

Param : V1.DC (V_V1.DC) = 7V

Specs : Max(I(M1:d)) = 431.46184192602732u

Simulation Run: 4

Param : V2.DC (V_V2.DC) = 10Vdc

Param : R3.VALUE (R_R3.Value) = 1k

Param : R4.Value (R_R4.Value) = 369 milliohms

Param : V1.DC (V_V1.DC) = 7.40000000000000

Specs : Max(I(M1:d)) = 479.00970366292034u

Simulation Run: 5

Param : V2.DC (V_V2.DC) = 9

Param : R3.VALUE (R_R3.Value) = 1.00400000000000k

Param : R4.Value (R_R4.Value) = 10.01422400000000

Param : V1.DC (V_V1.DC) = 6

Specs : Max(I(M1:d)) = 322.22565570185259u

Simulation Run: 6

Param : V2.DC (V_V2.DC) = 11

Param : R3.VALUE (R_R3.Value) = 996

Param : R4.Value (R_R4.Value) = 14.22400000000000m

Param : V1.DC (V_V1.DC) = 8

Specs : Max(I(M1:d)) = 554.67664021607891u

Sensitivity runs for various values in the circuit is provided in Table 3. As device geometry is made smaller, influence of drain dominates with that of the gate due to the growing proximity of the two electrodes, thereby increasing MOSFET sensitivity. Or in other words, the sensitivity of MOSFET current to drain voltage increases.

Table 3 – Values recorded for simulation runs with varying V1/V2/R3/R4 combinations and resulting drain current in micro amps

Simulation Run	V1 (V)	V2 (V)	R3 (K ohms)	R4 (milliohms)	Max(I(M1:d)) Micro amps
0	7	10	1	560	431.4618419
1	7	10.4	1	560	431.4618423
2	7	10	1.16	560	431.3817156
3	7	10	1	400	431.4618419
4	7	10.4	1	369	479.0097037
5	6	9	1.004	10.014	322.2256557
6	8	11	996	14.2	554.6766402

The plot between simulation run, R4 and Id shows the following relationship in Figure 14. The amplified currents are plotted, where the simulation would vary for temperature increase. The NPGF electrode surface would be varied from 0 to 70 degrees.

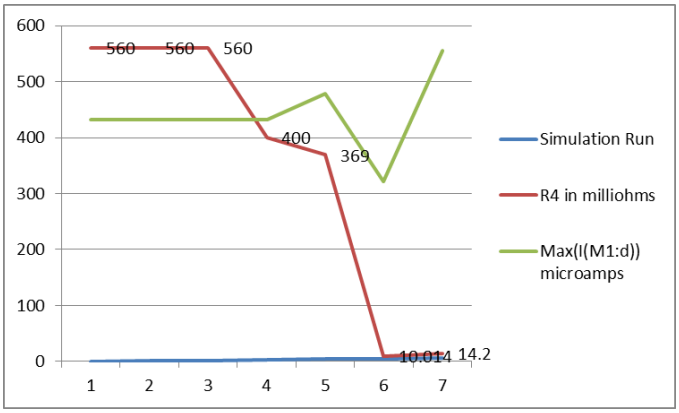

Figure 15 – Plot of R4 Vs Id relation

The signal to ratio variation is expected to be higher with NPGF used as variable resistor with MOSFET. Hence the transduction is expected to produce better sensitivity for testing ions. Figure 15 plots simulation runs for varied resistor values with maximum drain current plotted for different simulation runs.

C. Noise Analysis

The analysis of noise, as an effect of various components can be estimated using simulation. In the same context, the impact of variable resistor is analyzed for its noise factor in circuit. The magnitude of noise using only MOSFET structure with voltage sources and R3 is nil (for frequency range 0.1 to 100 k, whereas when variable resistance is used, a minimal noise magnitude of 9e-18 is measured. Noise measured in VNODE is 0.9e-18 out of MOSFET gate and the total noise is given as 9e-18. Hence the net contribution from passive components would be 8.1e-18. Considering the individual contributions it would be still lesser. The conclusion about signal to noise ratio connecting NPGF variable resistor to MOSFET drain node through VNODE is better compared to only MOSFET noise analysis. The

noise is measured for the parameters changed as in Table 3. The values are recorded for simulation runs with varying V1 or V2 or R3 or R4 combinations and resulting drain current in micro amps are recorded. Analysis is one for maximum drain current driven by MOSFET for average electrode area.

Noise in the presence of NPGF electrode :

To reduce iterations and even though MOSFTET configuration can be tracked for nodal performances using datasheets, the components and resistive component electrodes connected need to be analyzed for performances, particularly noise impact. The impact of noise magnitude upon adding nanoporous gold electrode as varying resistor with MOSFET is simulated. Two of the cases, one without variable resistor and another case with variable resistor are recorded. Instead of external noise, it is the inherent noise generated out of variable resistance operating with MOSFET.

A. Using only MOSFET

Figure 16 describes circuit model with MOSFET and power connections. Noise power is measured for MOSFET transducer circuit, where power spectral density can be described at room temperature Voltage spectral density is the square root of noise power spectral density. $3.312e^{-21}$ is the power spectral density measured.

Circuit model:

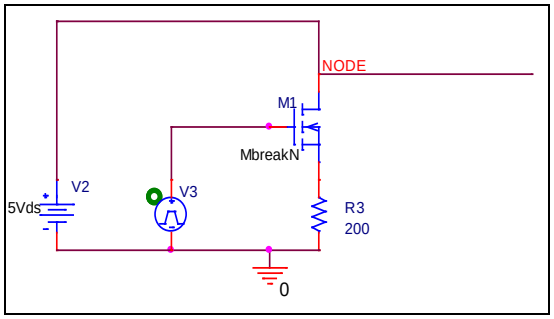

Figure 16: Circuit without Variable Resistor

Cadence simulated output:

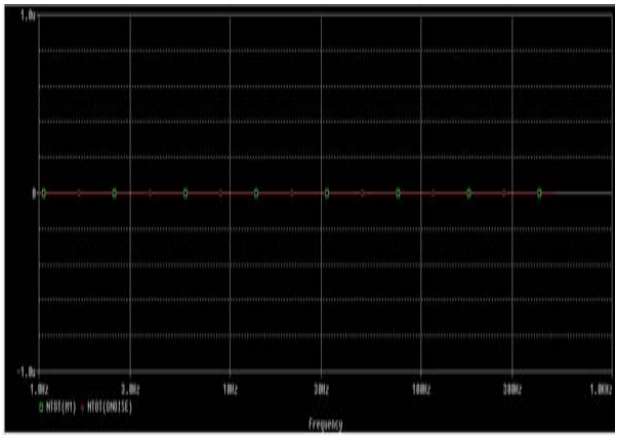

Figure 17: Graph for noise spectral power

Noise Magnitude is measured in volts and found to be nil, for the normalized drain current I_d/W, where I_d is the drain current for a given device geometry width. Decreasing size of MOSFET will increase signal performance. Noise optimization would be required based on the presence of noise. Primary contribution of noise in FETs include thermal noise and drain current / gate current. As gate current is very small, negligible current is estimated. Gate and noise current if present are independent of each other. If any device is connected between gate and drain, additional noises are generated, primarily white noise. Bulk noise in MOSFETs is due to the substrate layer interface, where in it can be reduced by biasing the bulk to minimize. Other noise sources include 1/f or flicker noise, noise in the resistive polygate, noise due to disturbed substrate resistance, shot noise due to leakage current of the drain source reverse diodes. Flicker noise can be eliminated by operating in low frequencies. For very low noise applications, the above noises are of consideration [23]. Most commonly thermal noise is of interest.

b. Using variable resistor

Circuit model describing with variable resistor connected in the drain node which is also powered using V4 is provided in Figure 18.

Circuit Model:

The noise model is designed such that an external noise is added to the circuit component using PSPICE, with the electrode in place. The resistor contributes noise in the form of random white noise, which can be measured to reduce it, based on the amount of presence.

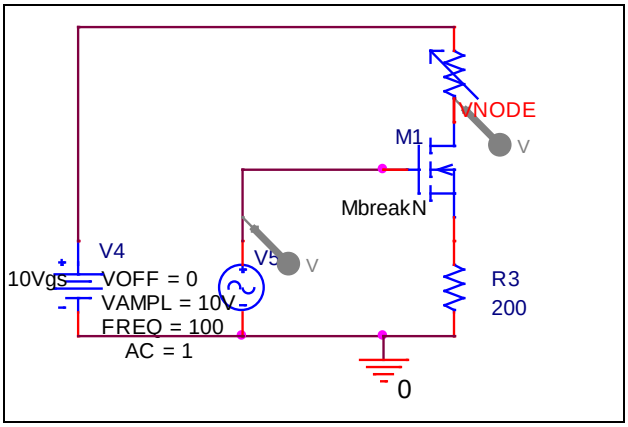

Figure 18: Noise analysis with variable resistor as NPGF electrode in place

Usually noise with resistor is added in series with the component. Power spectral density defines the noise power generated by a resistor in a particular bandwidth. Usually thermal noises in resistors occur due to random movement of carriers due to thermal excitation. Circuit design plays an important role in reducing such noise. Increasing signal to noise ratio can solve the noise problem.

$S = 4\ k\ T\ R$ (V2/Hz)

Where

S = Noise Power Spectral density
k = Boltzmans constant (1.38x10-23)
R = Resistance
T = Temperature in Kelvin
(Room temp = 27 °C = 300 K)

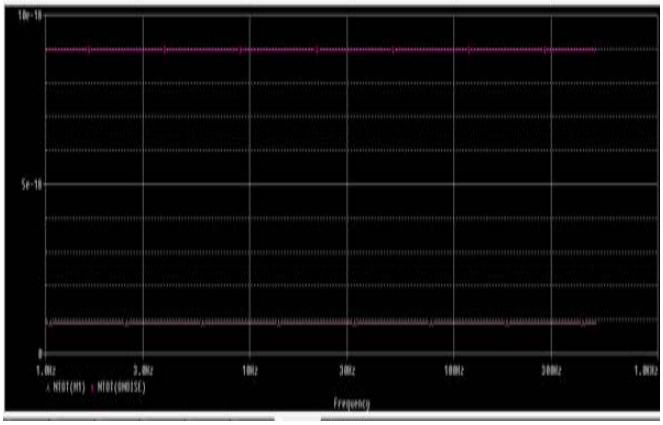

Figure 19: Output magnitude describing Mosfet noise=0.9e^{-18} whereas total output noise is 9e^{-18}. Net of 8.1e^{-18} is contributed through passive source.

Analyzing on the noise contribution sources, noises due to resistor contributes the major magnitude. The circuit is operated at lower frequency. The noise in MOSFETs are mostly frequency independent. If exists, it directly impacts the drain current noise in GHz range. The white noise is simulated as it is constant throughout the selected range of resistance. The spectral noise power is 6.11064e^{-21}, where the magnitude has increases with varying NPGF resistances over the surface area. The noise constant for n-MOSFET is 4x10^{-31} C^2/cm^2.

V. Conclusion

The Pspice simulation is performed for NPGF based MOSFET transducer for heavy metal ion sensing application. It proves that when the resistance varies through drain current, the output current amplification shows significant differences. The circuit is sensitive to electrode and varies according to resistance changes, changing the threshold voltage. Power dissipation and impact of noise is simulated.

References

[1] S. eds. Baldini, F., Chester, A.N., Homola, J. and Martellucci, Optical chemical sensors. Springer Science & Business Media., 2006. [2] J. Janata, Principles of chemical sensors. Springer Science & Business Media..,2010.

[3] S. Caetano and R. M. Ignácio, "World's largest Science , Technology & Medicine Open Access book publisher."

[4] Poomiapiradee, S., Brydson, R.M.D. and Kale, G.M., "Synthesis and Characterization of 2–3 Spinelsas Material for Methane Sensor.," Chem. Sensors Hostile Environ., p. pp.79-89,2002

[5] O. Korostynska, A. Mason, and A. Al-Shamma'a, "Monitoring of nitrates and phosphates in wastewater: Current technologies and further challenges," Int. J. Smart Sens. Intell. Syst., vol. 5, no. 1, pp. 149–176, 2012.

[6] K. Arshak, E. Moore, G. M. Lyons, J. Harris, and S. Clifford, "A review of gas sensors employed in electronic nose applications," Sens. Rev., vol. 24, no. 2, pp. 181–198, 2004.

[7] K. J. Albert, N. S. Lewis, C. L. Schauer, G. A. Sotzing, S. E. Stitzel, T. P. Vaid, and D. R. Walt, "Cross-reactive chemical sensor arrays," Chem. Rev. (Washington, DC, United States), vol. 100, no. 7, pp. 2595–2626, 2000.

[8] Baker, R.J., CMOS Circuit Design, Layout, and Simulation, Second Edition.,2008.

[9] S. Bhagavathula, J.M.Satchit, S. Roy Ramanan and Jegatha "Fabrication And Characterization of Electroless Plated Nanoporous Gold Film Electrode Electrode", International Conference on New Frontiers in Chemical, Energy and Environmental Engineering (INCEEE-2015), NIT Warangal, India, 2015.

[10] S. Joo and R. B. Brown, "Chemical Sensors with Integrated Electronics," Chem. Rev., vol. 108, no. 2, pp. 638–651, 2008.

[11] B. F. Myasoedov, "Chemical sensors (review)," Bull. Russ. Acad. Sci. Div. Chem. Sci., vol. 41, no. 3, pp. 383–387, Mar. 1992.

[12] D. M. Wilson, S. Hoyt, J. Janata, K. Booksh, and L. Obando, "Chemical sensors for portable, handheld field instruments," IEEE Sens. J., vol. 1, no. 4, pp. 256–274, 2001.

[13] J. Janata and M. Josowicz, "Conducting polymers in electronic chemical sensors," Nat. Mater., vol. 2, no. 1, pp. 19–24, 2003.

[14] M. Zayats, Y. Huang, R. Gill, C. A. Ma, and I. Willner, "Label-free and reagentless aptamer-based sensors for small molecules," J. Am. Chem. Soc., vol. 128, no. 42, pp. 13666–13667, 2006.

[15] S. Ready, F. Endicott, G. L. Whiting, T. N. Ng, E. M. Chow, and J. Lu, "3D Printed Electronics," 2013 Int. Conf. Digit. Print. Technol., pp. 9–12, 2013.

[16] A. Dodabalapur, "Organic and polymer transistors for electronics," Mater. Today, vol. 9, no. 4, pp. 24–30, 2006.

[17] E. Bakker and Y. Qin, "Electrochemical Sensors," Anal. Chem., vol. 78, no. 12, pp. 3965–3984, 2006.

[18] B.R.Eggins, Chemical sensors and biosensors, vol. 28, John Wiley & Sons, 2008.

[19] T. E. Edmonds, Chemical sensors. 1988.

[20] V. M. Mirsky, "Quantitative Characterization of Affinity Properties of Immobilized Receptors," Artif. Recept. Chem. Sensors, pp. 1–15, 2010.

[21] P. K. Yang, Ping and Chatterjee, "SPICE modeling for small geometry MOSFET circuits," IEEE Trans. Comput. Des. Integr. Circuits Syst., vol. 1, no. 4, pp. 169--182, 1982.

[22] S. Nasser, K. Bansal, and A. R. Kumar, "Modelling and 3D printing of Packaging for Water Quality Sensor."

[23] https://www.nikhef.nl/~jds/vlsi/noise/sansen.pdf